Joint Scheduling of Data Transmission and Wireless Power Transfer in Multi-Channel Device-to-Device Networks

Changhee Joo and Sunjung Kang

Abstract: **As the mobile traffic explodes, direct device-to-device communications attract much attention as one of next-generation technologies to increase the spatial spectrum efficiency in multi-channel wireless networks. On the other hand, as battery-powered mobile devices interrupt user experience due to limited battery capacity, wireless power transfer (WPT) has emerged as a convenient and perpetual power supply. However, current circuit technologies cannot support both energy harvesting and information decoding at the same time, and thus the Time-Division-Multiple-Access (TDMA) approach is often used for either data transmission or power transfer at a time, which requires joint scheduling of data transmissions and wireless power transfer. In this paper, we investigate the joint scheduling problem of multi-channel data transmissions and wireless power transfer, formulate the joint problem using a unified framework, and identify new difficulties in efficient resource allocation. We also develop a preliminary solution that achieves good empirical performance in single-hop D2D network scenarios.**

I. Introduction

Device-to-Device (D2D) communications have attracted much attention as a potential near-future solution to mobile traffic explosion. Through direct communications without traversing the base station or the access point, D2D communications can improve the spectral efficiency, energy efficiency, cellular coverage, delay performance, and fairness [1]. One of the main issues in D2D communication networks is the interference management. Since the cellular and D2D devices share the same frequency channel, their simultaneous transmissions may severely interfere with each other and none achieves an acceptable transmission rate. Power control [2] and successive interference cancellation technique [3], [4] have been employed to reduce the interference level of transmission signals, and several interference-aware resource allocation schemes have been designed to avoid simultaneous transmissions of nearby wireless links [5], [6]. In this work, we consider the problem of efficient resource allocation in multi-channel D2D networks, and investigate new aspects of resource allocation when the data transmission and wireless power transfer compete with each other.

Wireless Power Transfer (WPT) is a technology that delivers energy wirelessly from power sources to electrical loads. Since many mobile devices are powered by batteries, they should be recharged or replaced when their energy is depleted. Thus, as a convenient and perpetual power supply solution for mobile devices, WPT has attracted attention to replenish the energy over the air [7]. In practice, wireless power transfer is often implemented using one of three different technologies: inductive coupling, magnetic resonant coupling, and electromagnetic radiation (e.g., microwave power transfer (MPT)). Inductive and magnetic resonant coupling can be applied only for short range (less than a few meters), while MPT can be applied for long range (up to a few kilometers). It has been reported that beamed microwave power transmission can experimentally achieve the efficiency of 54% [8]. We consider MPT as wireless power transfer technology for mobile devices due to its long distance and efficiency. For higher efficiency, the power can be transferred from a shorter distance by densely deploying base stations or power beacons [7].

Recently, Simultaneous Wireless Information and Power Transfer (SWIPT) has been proposed and its rate-energy tradeoff has been studied on the assumption of simultaneous energy harvesting and information decoding [9]–[12]. However, in practice, the receiver cannot both harvest energy and decode the carried information at the same time [13], [14]. Two practical solutions have been proposed to this end: *time-switching*, for which the received signal is processed either for energy harvesting or for information decoding, and *power splitting*, for which the received signal is split into two signals of a fixed power ratio and each of them is used for energy harvesting and information decoding, respectively. Since the power splitting deteriorates the performance of power transfer and link capacity [14], we consider the time-switching model, where the information and the power are transmitted using the Time Division Multiple Access (TDMA) approach and each node can be involved either in data transmission or in power transfer at a time.

Numerous efficient scheduling schemes have been developed for TDMA-based data transmissions. Maximum Weight Scheduling (MWS) [15] has been shown to achieve the optimal throughput by computing the maximum weighted rate sum with weight of queue length. Despite its high performance, MWS has not been widely deployed in practice due to the requirement of centralized control and high computational complexity [16], which can cause significant amount of overhead in a large-scale D2D networks. Greedy Maximal Scheduling (GMS) (or Longest-Queue-First (LQF) scheduling) [17] that schedules the link with the largest weight first conforming to interference constraints, has a lower complexity and achieves good empirical performance, and thus can be considered an alternative solution in practice. Recently, Carrier Sense Multi-

Manuscript received May 14, 2016; approved for publication by XXX, June 08, 2016.

C. Joo is the corresponding author. This work is supported by IITP grant funded by the Korea government (MSIP) (No. B0126-16-1064, Research on Near-Zero Latency Network for 5G Immersive Service).

C. Joo and S. Kang are with the school of Electrical and Computer Engineering, UNIST, email: {cjoo, sky12382}@unist.ac.kr

ple Access (CSMA) based throughput-optimal scheduling algorithm has been developed [18], [19]. By sensing the channel before transmitting, each link coordinates its activity based on its own queue length, converging to the schedule distribution of an optimal solution. Although the CSMA algorithm achieves the optimal throughput performance, it suffers from poor delay performance in practice [20]. These scheduling schemes have been designed for data transmission in TDMA networks, and its extension to multi-channel wireless networks is straightforward since the channels can operate separately with each other. However, when the scheduling of multi-channel data transmissions that consume the battery energy is combined with the scheduling of wireless power transfer that replenishes the battery energy, the joint scheduling can be complicated and problematic since the transmissions at different channels are now coupled through the energy constraint.

In this work, we study the joint scheduling problem of multi-channel data transmissions and wireless power transfer. We identify the difficulties in high-performance joint scheduling with low computational complexity, and develop a practical solution that performs well in single-hop D2D network scenarios. We elaborate a unified framework of wireless scheduling for both data transmission and power transfer. Introducing energy shortage queues, we develop a shadow system that accommodates both data transmission and power transfer in a unified resource allocation problem of power deficiency transmission. We apply the previous schemes to the shadow system and identify their potential performance degradation. By modifying the greedy algorithms, we develop a practical solution to the joint scheduling of data transmission and wireless power transfer in D2D networks.

The rest of the paper is organized as follows. We introduce the system model for wireless data transmission and power transfer in Section II. We develop a unified model that can take into consideration both data transmission and wireless power transfer in Section III, and identify the problems of joint data transmission and power transfer under low-complexity scheduling schemes in Section IV. A solution that modifies GMS has been proposed in Section IV-C. We verify the performance of our solution through simulations in comparison with the other scheduling schemes in Section V, and conclude our paper in Section VI.

II. System Model

We consider a multi-channel wireless network modeled by a graph $G(N, L, F)$ with the set N of nodes, the set L of wireless links, and the set F of frequency channels. Each link can transmit over a single frequency channel $f(l) \in \{1, \ldots, M\}$ at a time, where transmissions at different frequency channel do not interfere with each other. We assume that each link has a unit capacity. Let $tx(l)$ and $rx(l)$ denote the transmitter and the receiver of link l, respectively.

Two links cannot transmit simultaneously at the same frequency channel if they interfere with each other. We employ the symmetric binary (or conflict) interference model: for links i and j, we define $C_{ij} \in \{0, 1\}$ as the interference relationship between links i and j, where $C_{ij} = C_{ji} = 1$ if they interfere with each other, and $C_{ij} = C_{ji} = 0$ otherwise. Note that if $C_{ij} = 1$, then $f(i) = f(j)$. We define the conflict set of link i as $C(i) = \{j \in L | C_{ij} = 1\}$.

We assume a time-slotted system. A (feasible) *transmission schedule* $\vec{S} \in \{0, 1\}^{|L|}$ is defined as the set of links that when they are active at the same time slot, no two links in the set interfere with each other. For each link l, we denote $S_l = 1$ or $l \in S$, if link l is included in schedule S, and $S_l = 0$ or $l \notin S$, otherwise. Let $\mathcal{S}$ be the set of all the transmission schedules. A transmission schedule is called *maximal* if no additional link can be added without violating the interference constraints. Let $\mathcal{M} \subset \mathcal{S}$ be the set of all the maximal schedules.

When a link is scheduled and make a data transmission, its transmitter consumes a fixed amount of energy, and cannot make further transmission if the energy storage is depleted. The energy can be replenished by wireless power transfer from base stations or power beacons using microwave radiation [7]. We assume that each node has an energy storage with infinite capacity, and that all the links with the same transmitter share the energy storage.

For scheduling the power transfer, we use the TDMA approach and avoid conflict with data transmissions, since a node cannot be involved in both data transmission and power transfer at the same time due to the restriction on the circuits [13], [14]. We assume that for each node, there is an associated base station or power beacon that delivers energy to the node through the beamed microwave power transmission. A base station or power beacon can be associated with multiple nodes, and uses directional antennas to prevent interference to and from other nodes [7]. Let $V_n(t) \in \{0, 1\}$ denote the activity of wireless power transfer of node n during time t. From our assumption, each link l should satisfy

$$S_l(t) + V_{tx(l)}(t) \leq 1 \text{ and } S_l(t) + V_{rx(l)}(t) \leq 1.$$

Let $\hat{V}_n$ be the unit of power transfer to node n from its associated power source during a time slot. Also let $\hat{U}_l$ be the unit of power consumption due to data transmission of link l. We specify how much energy has been consumed from the energy storage by *energy shortage queue* $P_n(t)$ of node n, which evolves as

$$P_n(t+1) = [P_n(t) - \hat{V} \cdot V_n(t)]^+ + \sum_{l:n=tx(l)} \hat{U}_l \cdot S_l(t). \quad (1)$$

In D2D communications, we consider the single-hop data traffic, i.e., the packets immediately leave the system once they are successfully transmitted. Let $A_l(t)$ be the number of packet arrivals at link l at the beginning of time slot t, which is upper-bounded by $\bar{A}$ and has mean $\lambda_l := E[A_l(t)]$. Let $Q_i(t)$ be the queue length at link l at the beginning of time slot t, which evolves as

$$Q_l(t+1) = [Q_l(t) - S_l(t) + A_l(t)]^+, \quad (2)$$

where $[\cdot]^+ := \max\{0, \cdot\}$. In the sequel, we omit the subscript t if there is no confusion.

A link is said to be *stable* if its queue length remains bounded, and the network is stable if all the links are stable and all the energy shortage queues are bounded. The *capacity region* is defined as the set of data arrival rates, for which some scheduling

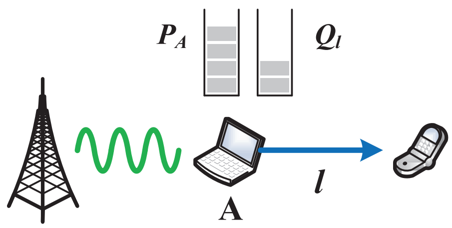

(a)Original network system

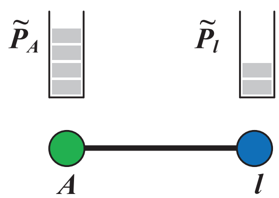

(b)Shadow system (conflict graph)

Fig. 1. Two representations of a network system with data transmission and wireless power transfer. In the original system, the wireless power transfer is shown as a wave and the data transmission is shown as a solid arrow. In the shadow system, the solid lines indicate the conflict relationship between the power deficiency queues.

policy can stabilize the network, and a scheduling policy is said to be *throughput-optimal* if it can stablilize the network for any arrival rate within the capacity region, by managing data queues and energy shortage queues properly.

III. Unifying Data Transmission and Wireless Power Transfer

In this section, we develop a resource allocation model that can combine both data transmission and wireless power transfer in a unified framework. The core idea is to convert data transmission and power transfer to a single power quantity, called power deficiency.

For ease of exposition, we consider a network that consists of one data link and one power transfer link as shown in Fig. 1(a). The transmitter A has energy shortage queue P_A, and link l has the data queue Q_l. For each component of the original network system, we construct a shadow system by mapping the wireless power transfer link at node A to vertex A and the data transmission link l to vertex l. When any two vertices cannot be active at the same time, we connect them by an edge, results in a *conflict graph* as shown in Fig. 1(b). Also we convert the energy shortage queue P_A of node A to the *power deficiency queue* $\tilde{P}_A$ of vertex A by setting $\tilde{P}_A = P_A$, and the data queue of link l to the power deficiency queue $\tilde{P}_l$ of vertex l by setting $\tilde{P}_l = \hat{U}_l \cdot Q_l$.

The shadow system is an image of the original system that operates as follows.

- When a data packet arrive at link l in the original system, the shadow system increase power deficiency queue $\tilde{P}_l$ by $\hat{U}_l$, which indeed equals to the amount of power to transmit the data packet through the link.
- When link l is scheduled and transmits a data packet in the original system, the corresponding vertex in the shadow system becomes active and transmit $\hat{U}_l$ unit power deficiency to the connected power transfer vertex A, i.e., $\hat{U}_l$ unit power deficiency moves from $\tilde{P}_l$ to $\tilde{P}_A$.
- When the sender of link l replenishes its battery through the wireless power transfer in the original system, the power deficiency queue $\tilde{P}_A$ of vertex A decreases by $\hat{V}_A$ in the shadow system.

Note that the above procedures maintain $\tilde{P}_A = P_A$ and $\tilde{P}_l = \hat{U}_l \cdot Q_l$ for all times. The power deficiency in the shadow system can be considered as the amount of energy needed to serve the data queues in the original system (i.e., similar to the energy shortage in the original system). Hence, it is clear that, if all the power deficiency queues in the shadow system remain finite, all the data queues and the energy shortage queues in the original system will remain finite, and vice versa. In this manner, the power deficiency allows us to have a unified view on the data transmission and the power transfer.

The joint problem of data transmission and wireless power transfer in the original system can be considered as the scheduling problem of 2-hop flows with fixed route in the shadow system: the power deficiency arrives at $\tilde{P}_l$, transmitted to $\tilde{P}_A$ by the data transmission of link l, and leaves the system by wireless power transfer to node A. We note that there is similarity between our model and that in [21], since both convert power or energy constraint to the queue structure. However, unlike [21], our model requires that the energy be explicitly replenished through wireless power transfer, which creates more complex structure involving multi-hop transmissions of the power deficiency.

We solve the 2-hop scheduling problem in the shadow queue and apply the scheduling decision to the original system. If the solution stabilizes the shadow system, it will also stabilize the original system. It has been shown that the Back-Pressure algorithm with *per-flow queues* solves the scheduling problem of multi-hop flows in a very general setting and achieve the optimal throughput [15]. However, the Back-Pressure algorithm cannot be directly applied to our case. Since the energy shortage queue P_n is shared by multiple data links whose transmitter is node n, the power deficiency queue $\tilde{P}_n$ are shared by all the flows that created by each data link in the shadow system. Thus the shadow system is per-vertex (or per-link) queue system by its construction.

Recently, Bo et al. show that the per-flow queues in the Back-Pressure scheme can be replaced with per-link queues under the condition that all the flows' routes do not form a loop [22]. Since the traffic is single-hop in the original system, the power deficiency of each flow in the shadow system starts from the vertex that represents the data link, e.g., l, goes through the vertex that represents the wireless power transfer to the transmitter of the data link, e.g., A, and leaves the system. Hence, i) all the flows are destined for one of the vertices for wireless power transfer, and ii) the destination vertices are not connected by an edge in the conflict graph, since multiple nodes can harvest energy at the same time thanks to the beamed microwave power transmission. These imply that the flows in the shadow system do not form a loop, and we can apply the Back-Pressure scheme with power deficiency queue in the shadow system. To elaborate, the

Back-Pressure scheme selects the set of vertices [15] such that

$$\vec{I} \in \operatorname{argmax} \sum_i \Delta \tilde{P}_i \cdot I_i, \tag{3}$$

subject to $I_i + I_j \leq 1$ for any two connected vertices i, j in the shadow system, where $I_i \in \{0, 1\}$, and

$$\Delta \tilde{P}_l := \begin{cases} \hat{U}_l \cdot (\tilde{P}_{rx(l)} - \tilde{P}_{tx(l)}) \text{ for data link } l \\ \hat{V}_n \cdot \tilde{P}_n \text{ for wireless power transfer link at node } n. \end{cases} \tag{4}$$

Proposition 1: For any arrival rate strictly within the capacity region, the above Back-Pressure scheme stabilizes the shadow system, and thus solves the joint problem of data transmission and wireless power transfer.
We omit the proof and refer to [22].

IV. Distributed Joint Scheduling

Although the Back-Pressure scheme achieves the optimal throughput performance, it requires centralized control and has high computational complexity to find the schedule that maximizes the queue weighted rate sum in the shadow system, which is known as an NP-Hard problem in general [16]. As the network scales up, the overhead will dominate and the algorithm cannot be implemented in practice. We consider the following low-complexity scheduling schemes as alternative practical solutions.

A. Greedy Maximal Scheduling

Greedy Maximal Scheduling (GMS) can be implemented in a distributed manner, has lower complexity $O(|E| \log |E|)$ [23], and empirically achieves the performance comparable to the Back-Pressure scheme [24]. It has been shown in [17] that GMS guarantees $\sigma(G)$-fraction of the optimal throughput where $\sigma(G)$ depends on the network topology. In the following, we show that GMS may suffer from performance degradation due to conflicts between data transmissions and wireless power transfers.

We first describe the GMS scheduling algorithm: starting with an empty set, it picks the link with the largest weight, adds to the set, and then excludes all the links that interfere with the link. The pick-add-exclude procedure repeats until there is no remaining link that is neither included in the set nor excluded. We extend the GMS algorithm to our 2-hop flow shadow system described in Section III, by setting the weight of a vertex in the shadow system as in (4).

Since data transmissions in different channels are non-interfering in our original system, it can be expected for GMS to achieve the same $\sigma(G)$ fraction of the optimal throughput. However, we will show that the performance of GMS may degrade since data transmissions in different channels compete through the shared energy shortage.

Let us consider an example network of two transmitters, each of which transmits data to two receivers through two frequency channels, as shown in Fig. 2(a). Let l_A and l_B denote the wireless power transfer links at node A and B, respectively. Let $l_{A,1}$ and $l_{A,2}$ denote the wireless D2D data links with transmitter A over channel 1 and 2, respectively. Similarly, let $l_{B,1}$ and $l_{B,2}$ denote the data links with transmitter B over channel 1 and 2, respectively. Suppose that the links of the same channel interfere with each other, e.g., $l_{A,1}$ and $l_{B,1}$ ($l_{A,2}$ and $l_{B,2}$, respectively) interfere with each other. In this sceanrio, it can be easily shown that GMS achieves the optimal throughput when there is no energy constraint [17].

Suppose that there are energy constraints, under which the power shortage queues at each node should remain finite. The wireless power transfer to a node interferes with all the data transmission links associated with the node, and there is no interference between wireless power transfers due to the beamed microwave power transmission through directional antennas. The interference relationship can be described by a conflict graph as shown in Fig. 2(b)

We assume that each data transmission consumes a unit of power, and the wireless power transfer provides two unit of power replenishment per slot, i.e., $\hat{U} = 1$ and $\hat{V} = 2$. Let $(A_{A,1}(t), A_{A,2}(t), A_{B,1}(t), A_{B,2}(t))$ denote the vector of data packet arrivals at link $(l_{A,1}, l_{A,2}, l_{B,1}, l_{B,2})$ at slot t in the original system. We consider the following packet arrival pattern, where the packets arrive at the beginning of each time slot. We start with an empty data queue for all the D2D links and empty energy shortage queues. At time 0, $(3, 4, 4, 3)$ packets arrive. After that, at each time t, one of the following sequence of packet arrivals occur.

1. With probability ϵ, $(4, 3, 3, 4)$ packet arrivals at t.
2. With probability ϵ, $(3, 4, 4, 3)$ packet arrivals at t.
3. With probability $(1 - 2\epsilon)$,
 $(1, 0, 0, 1)$ packet arrivals at t,
 $(0, 0, 0, 0)$ packet arrivals at $t + 1$,
 $(0, 1, 1, 0)$ packet arrivals at $t + 2$.

Ignoring the arrival at time 0, the mean arrival rate is

$$\begin{aligned} \vec{\lambda} &= \epsilon(4, 3, 3, 4) + \epsilon(3, 4, 4, 3) + (1 - 2\epsilon) \cdot (1, 1, 1, 1) \cdot \tfrac{1}{3} \\ &= \left(\tfrac{1}{3} + \tfrac{19}{3}\epsilon\right) \cdot (1, 1, 1, 1). \end{aligned} \tag{5}$$

Let us consider the shadow system under the above arrival pattern. If all the power deficiency queues remain finite, then the original system is stable. Let $\tilde{P}_A$ and $\tilde{P}_B$ denote the shared power deficiency queue of the vertex that represents the wireless power transfer to node A and node B, respectively. Also the power deficiency queue of the vertex that represents each data link is denoted by $\tilde{P}_{A,1}, \tilde{P}_{A,2}, \tilde{P}_{B,1}, \tilde{P}_{B,2}$, respectively as shown in Fig. 2(b).

Let $\mathcal{P} := (\tilde{P}_{A,1}, \tilde{P}_{A,2}, \tilde{P}_{B,1}, \tilde{P}_{B,2}, \tilde{P}_A, \tilde{P}_B)$ denote the vector of the power deficiency queues in the shadow system. Let $\mathcal{S} := (S_{A,1}, S_{A,2}, S_{B,1}, S_{B,2}, V_A, V_B)$ denote the vertex schedule of power deficiency in the shadow system. Note that $S_{A,1} \in \{0, 1\}$ corresponds to the data transmission of link $l_{A,1}$, and $V_A \in \{0, 1\}$ corresponds to the wireless power transfers at node A in the original system. Given the interference relationship between the power deficiency transmissions in the shadow system, we have 5 *maximal* schedules[1]:

$$(1, 0, 0, 1, 0, 0), (0, 1, 1, 0, 0, 0), (0, 0, 0, 0, 1, 1), \\ (1, 1, 0, 0, 0, 1), (0, 0, 1, 1, 1, 0).$$

Interleaving the above maximal schedules, we can characterize the capacity region. In particular, a static scheduling scheme that

[1]Maximal schedule is defined as a feasible schedule that cannot include additional transmission without violating the interference constraints.

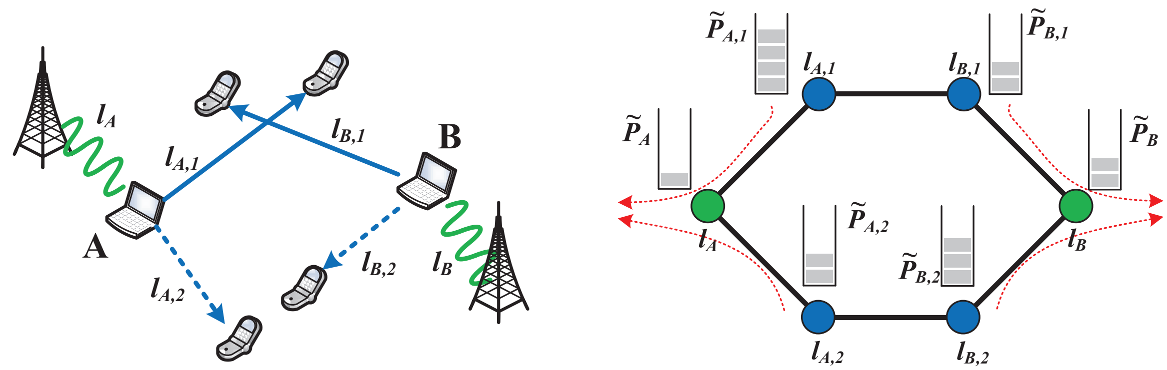

(a)Network graph of the original network system (b)Conflict graph of the corresponding shadow system

Fig. 2. Network graph of original system and shadow system. In the original system, the wireless power transfer is shown as green waves and the data transmissions in different frequency channels are shown as blue solid and dotted arrows. In the shadow system, the solid lines indicate the conflict relationship between the power deficiency queues and the dotted line denote the flows of the power deficiency.

interleaves two schedules of $(1,1,0,0,0,1)$ and $(0,0,1,1,1,0)$ with equal probability can stabilize the shadow system for the given $\vec{\lambda}$. Under this static scheme, the service rate of the power deficiency is

$$\tfrac{1}{2}(\hat{U},\hat{U},0,0,0,\hat{V})+\tfrac{1}{2}(0,0,\hat{U},\hat{U},\hat{V},0)=\left(\tfrac{1}{2},\tfrac{1}{2},\tfrac{1}{2},\tfrac{1}{2},1,1\right).$$

Since the service rate of vertices l_A and l_B is no smaller than the service rate sum of $l_{A,1}$ and $l_{A,2}$, and $l_{B,1}$ and $l_{B,2}$, respectively (that is, $1=\hat{V}\cdot V_n \geq S_{n,1}+S_{n,2}=\frac{1}{2}+\frac{1}{2}$, for $n\in\{A,B\}$), the deficiency queues $\tilde{P}_A$ and $\tilde{P}_B$ will remain finite.

For other vertices, the service rate of the power deficiency queue is no smaller than the arrival rate, i.e., $\frac{1}{2}=S_k\geq\hat{U}\cdot\lambda_k\approx\frac{1}{4}$, for all $k\in\{l_{A,1},l_{A,2},l_{B,1},l_{B,2}\}$. Therefore, the static scheduling scheme can successfully support the given $\vec{\lambda}$ for any $\epsilon>0$.

We now investigate the performance of GMS with weight (4) in the shadow system. Suppose that at the beginning of time t, the power deficiency queue is $(3K,3K,3K,3K,K,K)$ for some integer $K\geq 1$. Given the traffic pattern of $\vec{\lambda}$, we show that under GMS, the queue lengths remain $(3K,3K,3K,3K,K,K)$ with probability $(1-2\epsilon)$, and increase to $(3(K+1),3(K+1),3(K+1),3(K+1),K+1,K+1)$ with probability 2ϵ. Table 1 illustrates the evolution of the power deficiency queues and the schedules of GMS for the given traffic pattern. Note that the schedules of GMS are determined by choosing first the link with the largest weight, and the weight is computed as in (4) with $\hat{U}=1,\hat{V}=2$.

The result shows that once the queues are $(3K,3K,3K,3K,K,K)$ for any $K\geq 1$, they keep increasing under GMS for the given traffic $\vec{\lambda}$. What remains to show is that the power deficiency queue becomes $(3,3,3,3,1,1)$ at some time since time 0. Considering the packet arrival at time 0, i.e., when $(3,4,4,3,\cdot,\cdot)$ packets arrive at the empty queues at the beginning of time 0, the weight in the shadow system is $(3,4,4,3,0,0)$ and thus links $l_{A,2}$ and $l_{B,1}$ will be scheduled by GMS. At the end of time 0, the power deficiency queues in the shadow system become $(3,3,3,3,1,1)$, which completes our proof.

Therefore, the given traffic $\vec{\lambda}$, the power deficiency queues keep increasing with any $\epsilon>0$ under GMS. Since the static scheduling scheme achieves up to $\frac{1}{2}(1,1,1,1)$, GMS can achieve no greater than $\frac{2}{3}$ fraction of the optimal performance. Since $\sigma(G)=1$ in the original system (without energy constraints). Our result show that in multi-channel networks with wireless power transfer, GMS cannot guarantee $\sigma(G)$ fraction of the capacity region. Finally, we remark that the coupling of the data transmissions in different channels is not because the wireless power transfer that interfere with all the data transmissions across the channels, but rather because they share the power deficiency queue (energy shortage queue).

B. CSMA-based Joint Scheduling

Another alternative method is to apply CSMA-based schemes to the shadow system. CSMA-based scheduling schemes with weight (4) have been shown to be optimal in multi-hop wireless networks [18]. Hence, we can extend their results to the shadow system. To elaborate, we modify discrete-time scheduling of Q-CSMA [19] as follows.

We can obtain the following proposition.

Proposition 2: CSMA-based joint scheduling scheme for the shadow system can achieve the optimal throughput performance by setting

$$p_i=\frac{\Delta\tilde{P}_i}{\Delta\tilde{P}_i+1}.$$

The proposition can be shown using the similar techniques of [18], [19]. Since the scheme schedules the links of the close-to-maximum weight sum with the weight defined in (4), its stability for any arrival rate in the capacity region can be shown using the Lyapunov technique. For the completeness, we provide the detailed proof in Appendix.

Although CSMA-based scheduling scheme is throughput-optimal, it empirically suffers from poor delay performance, as shown later in Section V.

C. A Heuristic Modification to GMS

In this section, we develop a heustic modification to GMS scheduling scheme to enhance its performance. In addition to basic GMS algorithm, we add the following rules.

- If a data link l is chosen by the greedy algorithm, then for the next selection, a priority is given to the data link that shares the

Table 1. Evolution of the power deficiency queues of the shadow system under GMS for the given arrival pattern. ($\hat{U} = 1, \hat{V} = 2$)

Traffic pattern	Time	Power Deficiency Queue Changes	
Case 1: With prob.ϵ	t	Initial queue length	$(3K, 3K, 3K, 3K, K, K)$
		Arrival	$(4, 3, 3, 4, \cdot, \cdot)$
		Weight	$(2K + 4, 2K + 3, 2K + 3, 2K + 4, 2K, 2K)$
		Schedule	$(1, 0, 0, 1, 0, 0)$
		Final queue length	$(3(K + 1), 3(K + 1), 3(K + 1), 3(K + 1), K + 1, K + 1)$
Case 2: With prob.ϵ	t	Initial queue length	$(3K, 3K, 3K, 3K, K, K)$
		Arrival	$(3, 4, 4, 3, \cdot, \cdot)$
		Weight	$(2K + 3, 2K + 4, 2K + 4, 2K + 3, 2K, 2K)$
		Schedule	$(0, 1, 1, 0, 0, 0)$
		Final queue length	$(3(K + 1), 3(K + 1), 3(K + 1), 3(K + 1), K + 1, K + 1)$
Case 3: With prob. $(1 - 2\epsilon)$	t	Initial queue length	$(3K, 3K, 3K, 3K, K, K)$
		Arrival	$(1, 0, 0, 1, \cdot, \cdot)$
		Weight	$(2K + 1, 2K, 2K + 1, 2K, 2K, 2K)$
		Schedule	$(1, 0, 0, 1, 0, 0)$
		Final queue length	$(3K, 3K, 3K, 3K, K + 1, K + 1)$
	t+1	Initial queue length	$(3K, 3K, 3K, 3K, K + 1, K + 1)$
		Arrival	$(0, 0, 0, 0, \cdot, \cdot)$
		Weight	$(2K - 1, 2K - 1, 2K - 1, 2K - 1, 2(K + 1), 2(K + 1))$
		Schedule	$(0, 0, 0, 0, 1, 1)$
		Final queue length	$(3K, 3K, 3K, 3K, K - 1, K - 1)$
	t+2	Initial queue length	$(3K, 3K, 3K, 3K, K - 1, K - 1)$
		Arrival	$(0, 1, 1, 0, \cdot, \cdot)$
		Weight	$(2K + 1, 2K + 2, 2K + 2, 2K + 1, 2(K - 1), 2(K - 1))$
		Schedule	$(0, 1, 1, 0, 0, 0)$
		Final queue length	$(3K, 3K, 3K, 3K, K, K)$

Algorithm 1 CSMA-based joint scheduling.

Control slot: select a decision schedule $\vec{d} \in \mathcal{M}$ with probability $\alpha(\vec{d}(t))$.
for $i \in \vec{d}(t)$ **do**
  if $\sum_{j \in \mathcal{C}(i)} S_j(t-1) = 0$ **then**
    $S_i(t) = 1$ with probability p_i;
    $S_i(t) = 0$ with probability $\bar{p}_i = 1 - p_i$.
  else
    $S_i(t) = 0$.
  end if
end for
for $i \notin \vec{d}(t)$ **do**
  $S_i(t) = S_i(t-1)$.
end for

Data slot: for each $l \in \vec{S}(t)$, link l transmits data if it is for the data transmission, and link l transfers power if it is for the power transfer.

same power queue with link l. If there are multiple such links that interfere with each other, then the link with larger weight will be chosen first.
For example, if link $l_{A,1}$ is chosen first by the greedy algorithm, the next selection priority is given to link $l_{A,2}$.

We model our previous example to a system with 4 queues in tandem (linear topology), where any two neighboring queues cannot be in service at the same time, as shown in Fig. 3.

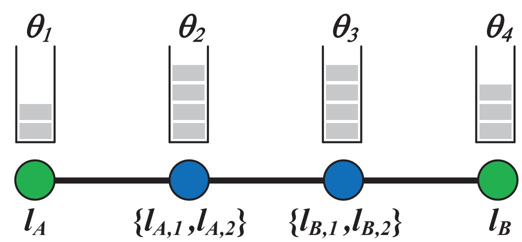

Fig. 3. Tandem queue system with 4 queues.

The queues of the new system are denoted by $\theta_1, \theta_2, \theta_3, \theta_4$, and set as $\theta_1(t) = \tilde{P}_A(t)$, $\theta_2(t) = \max\{\tilde{P}_{A,1}(t), \tilde{P}_{A,2}(t)\}$. $\theta_3(t) = \max\{\tilde{P}_{B,1}(t), \tilde{P}_{B,2}(t)\}$, and $\theta_4 = \tilde{P}_B(t)$. Our modified GMS, denoted by GMS for Power Transfer (GMS-PT) can be considered as GMS scheduling in this tandem queue system, except the following two schedules

$$(1, 0, 0, 1, 0, 0) \text{ and } (0, 1, 1, 0, 0, 0),$$

i.e., the cases that two different data links with different channel are scheduled. In such cases, the corresponding schedule in the tandem queue will be $(0, 1, 1, 0)$, which is not feasible in our tandem queue model. All other feasible schedules in the shadow system, can be mapped to a feasible schedule in the tandem queue model.

It has been well known that GMS achieves the capacity region in this tandem system [17]. However, the capacity region of our

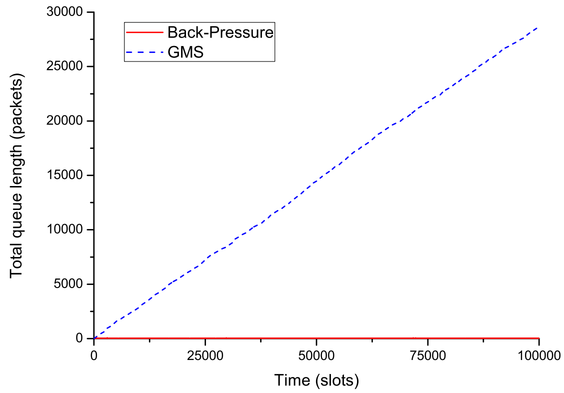

Fig. 4. Performance of Back-Pressure and GMS.

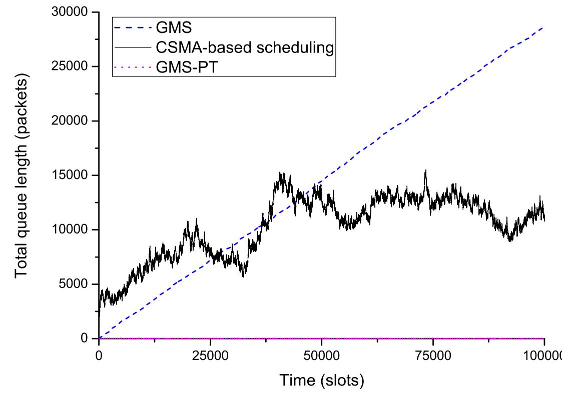

Fig. 5. Performance of GMS, CSMA-based scheduling, and GMS-PT.

tandem queue model is different from that of our shadow system due to the missing schedules. For the tandem queue model, the capacity region can be described as

$$\{\vec{\lambda}\,|\frac{\lambda_{\theta_1}}{\hat{V}_A}+\lambda_{\theta_2}\leq 1,\lambda_{\theta_2}+\lambda_{\theta_3}\leq 1,\lambda_{\theta_3}+\frac{\lambda_{\theta_4}}{\hat{V}_B}\leq 1\} \qquad (6)$$

where $\lambda_{\theta_1} = \lambda_A, \lambda_2 = \max\{\lambda_{A,1},\lambda_{A,2}\}, \lambda_3 = \max\{\lambda_{B,1},\lambda_{B,2}\}, \lambda_{\theta_4} = \lambda_B$. The performance of GMS-PT can be characterized by comparing (6) with the capacity region of the shadow system, which remains as an interesting open problem.

V. Numerical Result

We evaluate the performance of joint scheduling of data transmission and wireless power transfer through simulations. We apply the Back-Pressure, GMS, CSMA, and GMS-PT schemes to the shadow system, and trace their queue length evolution. We use the topology, network settings, and the arrival pattern described in in Section IV with $\epsilon = 0.05$ ($\hat{U} = 1$, $\hat{V} = 2$, and $\vec{\lambda} = \left(\frac{1}{3} + \frac{13}{3}\epsilon\right) \cdot (1, 1, 1, 1)$).

Fig. 4 shows the total queue lengths of the Back-Pressure and GMS schemes. Although the Back-Pressure supports the arrival rate and maintains the queue length low (overlapped with the x-axis in the figure), GMS fails to support the arrival rate and has the queue lengths that keep increasing linearly in time. Fig. 5 illustrates the queue length trace of CSMA-based joint scheduling and GMS-PT. The results of GMS has been included as the reference. Although both CSMA-based scheme and GMS-PT successfully accommodate the arrival rate and has finite queue lengths, the CSMA-based scheme has a large number of queue lengths and thus suffers from poor delay performance. In contrast, GMS-PT achieves as low queue lengths (< 50) as the Back-Pressure scheme.

VI. Conclusion

We have investigated the joint scheduling problem of data transmission and wireless power transfer in multi-channel D2D networks. We develop a unified framework that combines the two different transmission scheduling into one using energy queues, and show that data transmissions can be done in an energy-efficient fashion. We identify that the combined energy queues can cause unexpected coupling between non-interfering channels, which results in scheduling inefficiency. By modifying the greedy scheduling, we design a heuristic joint scheduling scheme. Through numerical results, we show that the proposed scheme performs as well as the centralized Back-Pressure algorithm.

REFERENCES

[1] A. Asadi, Q. Wang, and V. Mancuso, “A Survey on Device-to-Device Communication in Cellular Networks,” IEEE Communications Surveys & Tutorials, vol.16, no.4, pp. 1801-1819, 2014.
[2] B. Kaufman and B. Aazhang, “Cellular Networks with an Overlaid Device to Device Network,” 42nd Asilomar Conference on Signals, Systems and Computers, pp.1537-1541, Oct. 2008.
[3] C. Nam, C. Joo, S-G. Yoon, and S. Bahk, “Resource Allocation in Full-Duplex OFDMA Networks: Approaches for Full and Limited CSIs,” to appear in Journal of Communications and Networks.
[4] C. Yu and O. Tirkkonen, “Device-to-Device Underlay Cellular Network based on Rate Splitting,” IEEE Wireless Communications and Networking Conference (WCNC), April 2012.
[5] H. Min, J. Lee, S. Park, and D. Hong, “Capacity Enhancement Using an Interference Limited Area for Device-to-Device Uplink Underlaying Cellular Networks,” IEEE Transactions on Wireless Communications, vol.10, no.12, pp.3995-4000, December 2011.
[6] R. Zhang, X. Cheng, L. Yang, and B. Jiao, “Interference-aware Graph based Resource Sharing for Device-to-Device Communications Underlaying Cellular Networks,” IEEE Wireless Communications and Networking Conference (WCNC), April 2013.
[7] K. Huang and V. K. N. Lau, “Enabling Wireless Power Transfer in Cellular Networks: Architecture, Modeling and Deployment,” IEEE Transactions on Wireless Communications, vol. 13, no. 2, pp. 902-912, February 2014.
[8] W. C. Brown and E. E. Eves, “Beamed microwave power transmission and its application to space,” IEEE Transactions on Microwave Theory and Techniques, vol.40, no.6, pp.1239-1250, Jun 1992.
[9] L. R. Varshney, “Transporting information and energy simultaneously,” in Proc. IEEE ISIT, pp. 1612-1616, Jul. 2008.
[10] P. Grover and A. Sahai, “Shannon meets Tesla: wireless information and power transfer,” in Proc. IEEE ISIT, pp. 2363-2367, Jun. 2010.
[11] J. Park and B. Clerckx, “Joint Wireless Information and Energy Transfer in a Two-User MIMO Information Channel,” IEEE Transactions on Wireless Communications, vol.12, no.8, pp. 4210-4221, Aug. 2013.
[12] Y. Xiao, D. Niyato, Z. Han, and L. A. DaSilva, “Joint Optimization for Power Scheduling and Transfer in Energy Harvesting Communications,” in Proc. IEEE Globecom, 2015.
[13] R. Zhang and C. K. Ho, “MIMO Broadcasting for Simultaneous Wireless Information and Power Transfer,” IEEE Globecom, 2011.
[14] X. Zhou, R. Zhang, and C. K. Ho, “Wireless Information and Power Transfer in Multiuser OFDM Systems,” IEEE Transactions on Wireless Communications, vol.13, no.4, pp.2282-2294, April 2014.
[15] L. Tassiulas and A. Ephremides, “Stability Properties of Constrained

Queueing Systems and Scheduling Policies for Maximal Throughput in Multihop Radio Networks," IEEE Transactions on Automatic Control, vol. 37, no. 12, pp. 1936-1948, December 1992.

[16] C. Joo, G. Sharma, and N. B. Shroff, and R. R. Mazumdar, "On the Complexity of Scheduling in Wireless Networks," EURASIP Journal of Wireless Communications and Networking, Oct. 2010.

[17] C. Joo, X. Lin, and N. B. Shroff, "Understanding the Capacity Region of the Greedy Maximal Scheduling Algorithm in Multi-hop Wireless Networks," IEEE/ACM Transactions on Networking, vol. = 17, no. 4, Aug. 2009.

[18] L. Jiang and J. Walrand, "A Distributed CSMA Algorithm for Throughput and Utility Maximization in Wireless Networks," IEEE/ACM Transactions on Networking, vol.18, no.3, pp.960,972, June 2010.

[19] J. Ni, B. Tan, R. Srikant, "Q-CSMA: Queue-Length Based CSMA/CA Algorithms for Achieving Maximum Throughput and Low Delay in Wireless Networks," IEEE/ACM Transactions on Networking, vol. 20, no. 3, June 2012.

[20] Changhee Joo, "On Random Access Scheduling for Multimedia Traffic in Multi-hop Wireless Networks with Fading Channels," IEEE Transactions on Mobile Computing (TMC), vol. 12, no. 4, pp. 647656, April 2013.

[21] M. J. Neely, "Energy Optimal Control for Time-Varying Wireless Networks," IEEE Transactions on Information Theory, vol.52, no.7, July 2006.

[22] B. Ji, C. Joo, and N. B. Shroff, "Throughput-Optimal Scheduling in Multihop Wireless Networks Without Per-Flow Information," IEEE/ACM Transactions on Networking, vol. 21, no. 2, April 2013.

[23] J. Hoepman, "Simple Distributed Weighted Matchings," eprint, http://arxiv.org/abs/cs/0410047v1, Oct. 2004.

[24] C. Joo and N. B. Shroff, "Performance of Random Access Scheduling Schemes in Multi-hop Wireless Networks," IEEE/ACM Transactions on Networking, vol. 17, no. 5, October 2009.

[25] A. Eryilmaz, R. Srikant, and J. R. Perkins, "Stable Scheduling Policies for Fading Wireless Channels," vol. 13, no. 2, pp. 411-424, 2005.

Appendix

Proof of Proposition 2

It can be easily shown that the DTMC of the transmission schedule is irreducible and aperiodic. Suppose that the stationary distribution of the algorithm is

$$\pi(\vec{S}) = \frac{1}{Z}\prod_{l\in\vec{S}}\frac{p_l}{\bar{p_l}}, \quad \text{where } Z = \sum_{\vec{S}\in\mathcal{M}}\prod_{l\in\vec{S}}\frac{p_l}{\bar{p_l}}. \tag{7}$$

If the following local balance equation holds for any two states $\vec{S}$ and $\vec{S'}$, then (7) is indeed the stationary distribution of the algorithm from the reversibility of the DTMC.

$$\pi(\vec{S})P(\vec{S},\vec{S'}) = \pi(\vec{S'})P(\vec{S'},\vec{S}), \tag{8}$$

where

$$P(\vec{S},\vec{S'}) = \sum_{\vec{d}\in\mathcal{M}}\alpha(\vec{d})\cdot\Big(\prod_{l\in\vec{S}\setminus\vec{S'}}\bar{p_l}\Big)\cdot\Big(\prod_{k\in\vec{S'}\setminus\vec{S}}p_k\Big) \cdot\Big(\prod_{i\in\vec{d}\cap(\vec{S}\cap\vec{S'})}p_i\Big)\cdot\Big(\prod_{j\in\vec{d}\setminus(\vec{S}\cup\vec{S'})\setminus\mathcal{C}(\vec{S}\cup\vec{S'})}\bar{p_j}\Big). \tag{9}$$

Then the left side of (8) can be derived as

$$\begin{aligned}\pi(\vec{S})P(\vec{S},\vec{S'}) &= \frac{1}{Z}\Big(\frac{\prod_{l\in\vec{S}}p_l}{\prod_{l\in\vec{S}}\bar{p_l}}\Big)\cdot\sum_{\vec{d}\in\mathcal{M}}\alpha(\vec{d})\cdot\Big(\frac{\prod_{l\in(\vec{S}\cup\vec{S'})}\bar{p_l}}{\prod_{l\in\vec{S'}}}\Big)\\ &\cdot\Big(\frac{\prod_{k\in(\vec{S}\cup\vec{S'})}p_k}{\prod_{k\in\vec{S}}p_k}\Big)\cdot\Big(\prod_{i\in\vec{d}\cap(\vec{S'}\cap\vec{S})}p_i\Big)\\ &\cdot\Big(\prod_{j\in\vec{d}\setminus(\vec{S'}\cup\vec{S})\setminus\mathcal{C}(\vec{S'}\cup\vec{S})}\bar{p_j}\Big)\cdot\Big(\frac{\prod_{a\in\vec{S'}}p_a}{\prod_{a\in\vec{S'}}p_a}\Big)\\ &= \frac{1}{Z}\prod_{l\in\vec{S'}}\frac{p_l}{\bar{p_l}}\cdot\sum_{\vec{d}\in\mathcal{M}}\alpha(\vec{d})\cdot\Big(\prod_{l\in\vec{S'}\setminus\vec{S}}\bar{p_l}\Big)\\ &\cdot\Big(\prod_{k\in\vec{S}\setminus\vec{S'}}p_k\Big)\cdot\Big(\prod_{i\in\vec{d}\cap(\vec{S'}\cap\vec{S})}p_i\Big)\cdot\Big(\prod_{j\in\vec{d}\setminus(\vec{S'}\cup\vec{S})\setminus\mathcal{C}(\vec{S'}\cup\vec{S})}\bar{p_j}\Big)\\ &= \pi(\vec{S'})P(\vec{S'},\vec{S}),\end{aligned} \tag{10}$$

which equals to the right side. Now we show that the CSMA-based joint scheduling achieves throughput optimal from the stationary distribution (7). Let us define the link weight $w_i(t) = f_i(\Delta\tilde{P}_i(t))$ for $i\in E$, where $\Delta\tilde{P}_i(t)$ is the queue length differential to the next hop, $f_i(q)\in\mathbb{R}^+$ is a non-decreasing continuous function with $\lim_{q\to\infty}f_i(q)=\infty$. Also for any $M_1>0, M_2>0$, and $0<\epsilon<1$, there exists $Q<\infty$ such that

$$(1-\epsilon)f_i(q)\le f_i(q-M_1)\le f_i(q+M_2)\le(1+\epsilon)f_i(q),$$

for all $q>Q$. Choose the link activation probability p_i (in line 4 and 5 in Algorithm 1) as

$$p_i = \frac{e^{w_i(t)}}{e^{w_i(t)}+1}.$$

For example, we set $f_i(q)=\log q$. Given any ϵ and δ, where $0<\epsilon,\delta<1$, we define a set

$$\mathcal{X} := \{\vec{S}\in\mathcal{M}:\sum_{i\in\vec{S}}w_i(t)<(1-\epsilon)w^*(t)\}, \tag{11}$$

where $w^*(t) := \max_{\vec{S}\in\mathcal{M}}\sum_{i\in\vec{S}}w_i(t)$, then

$$\begin{aligned}\pi(\mathcal{X}) &= \sum_{\vec{S}\in\mathcal{X}}\pi(\vec{S}) = \sum_{\vec{S}\in\mathcal{X}}\frac{1}{Z}\prod_{i\in\vec{S}}\frac{p_i}{\bar{p_i}}\\ &= \sum_{\vec{S}\in\mathcal{X}}\frac{1}{Z}\prod_{i\in\vec{S}}e^{w_i(t)} = \sum_{\vec{S}\in\mathcal{X}}\frac{e^{\sum_{i\in\vec{S}}w_i(t)}}{Z}\\ &\le \sum_{\vec{S}\in\mathcal{X}}\frac{e^{(1-\epsilon)w^*(t)}}{Z} \le \frac{|\mathcal{X}|e^{(1-\epsilon)w^*(t)}}{Z}\\ &< \frac{2^{|E|}}{e^{\epsilon w^*(t)}},\end{aligned} \tag{12}$$

where the last inequality comes from the fact that $|\mathcal{X}|\le|\mathcal{M}|\le 2^{|E|}$ and $Z>e^{\max_{\vec{S}\in\mathcal{M}}\sum_{i\in\vec{S}}w_i(t)}=e^{w^*t}$. Hence, if

$$w^*(t) > \frac{1}{\epsilon}(|E|\log 2+\log\frac{1}{\delta}), \tag{13}$$

then we have $\pi(\mathcal{X}) < \delta$. Since $w^*(t)$ is a non-decreasing continuous function of $\tilde{P}_i(t)$ with $\lim_{||\tilde{P}_i|| \to \infty} w^*(t) = \infty$, there exists $B > 0$ such that (13) is satisfied whenever $||\tilde{P}_i|| > B$. This implies that when $\tilde{P}_i$ is large enough, the stationary distribution, $\pi(\vec{S})$, converges to the set $\mathcal{X}^c = \mathcal{M} \backslash \mathcal{X}$ with high probability (i.e., $\pi(\mathcal{X}^c) \geq 1 - \delta$). From the fact that for a scheduling algorithm, if for any ϵ and δ, $0 < \epsilon, \delta < 1$, there exists a $B > 0$ such that in any time slot t, with probability greater than $1 - \delta$, the scheduling algorithm chooses a schedule $\vec{S} \in \mathcal{M}$ satisfying

$$\sum_{i \in \vec{S}} w_i(t) \geq (1 - \epsilon) \max_{\vec{S} \in \mathcal{M}} \sum_{i \in \vec{S}} w_i(t), \tag{14}$$

whenever $||\tilde{P}_i|| > B$. Then the throughput optimality of the scheduling algorithm can be shown by using the Lyapunov technique with a quadratic weight sum function as in [25].

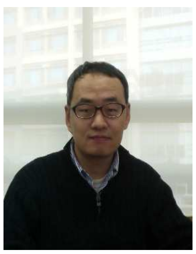

Changhee Joo received his Ph.D. degree from Seoul National University, Korea. Since 2005, he was with Purdue University and the Ohio State University, and joined Korea University of Technology and Education, Korea, in 2010. He is now with UNIST, Korea. His research interests include resource allocation in wireless networks, network optimization, wireless sensor networks, and Internet protocols. He is an editor of the Journal of Communications and Networks and has served for several primary conferences as a committee member, including the Institute of Electrical and Electronics Engineers (IEEE) International Conference on Communications (INFOCOM), the IEEE Communications Society Conference on Sensing, Communication, and Networking (SECON), and the Association for Computing Machinery (ACM) Symposium on Mobile Ad Hoc Networking and Computing (MobiHoc). Dr. Joo is a recipient of the IEEE INFOCOM 2008 best paper award, the ICTC 2015 best paper award, and the Korean Institute of Communications and Information Sciences (KICS) Haedong Young Scholar Award (2014).

Sunjung Kang received her B.S. degree from the school of ECE at Ulsan National Institute of Science and Technology (UNIST) in 2016. She is currently an M.S. student in the school of ECE at UNIST. Her research interests include resource allocation and cognitive radio networks.